Kasetsart J. (Nat. Sci.) 47 : 101 - 114 (2013)

Biosorption of Local Textile Dyes Onto Acid-Tolerant Macro-Beads of Chitosan-Immobilized *Rhizopus arrhizus* Biomass

Weeranuch Lang[1, 2], Pitchpong Buakaew [3], Wanvisa Buranaporipan[4], Jintanart Wongchawalit[2], Nobuo Sakairi[4], Wirat Vanichsriratana[5, 6] and Sarote Sirisansaneeyakul[5, 6,*]

ABSTRACT

Industrial textile dye removal was investigated using dried fungal biomass (FB) and acid-tolerant chitosan-immobilized *Rhizopus arrhizus* biomass (Ch-F beads) to elucidate their potential application. The biosorption of two textile dyes, Cibacron Turquoise HGN (CT) and Remazol Red RGB (RR) was tested as dye models for phthalocyanine-based and azo-based reactive dyes. The surface charge density of Ch-F beads and FB was found to strongly accumulate both dyes under similar acidic (pH 3.0) conditions because of the synergy between the positive charges of the acidic pH and the anionic reactive dyes. The role of physicochemical properties related to their biosorption was described. Biosorption equilibrium was established within 30 min for the FB, but retarded for the Ch-F beads due to the densely packed fungal mycelia inside the beads. The diffusivity of RR and CT in the biosorbent was verified exploiting the proposed intraparticle diffusion model. According to the Langmuir model, the maximum dye uptake capacity of the Ch-F beads for RR and CT was 198.15 and 76.84 $mg.g^{-1}$, respectively. The desorption of dye-loaded Ch-F was effective using 0.1 M NaOH. This indicated the desirable applicability of Ch-F beads for the treatment of wastewaters containing dyes.

Keywords: chitosan, biosorption, textile dyes, *Rhizopus arrhizus*, isotherm, acid

INTRODUCTION

Chitosan, (1→4)-2-amino-2-deoxy-β-D-glucan, is a multifunctional polymer that is regarded as a useful starting material for various purposes, such as an ion exchanger (Riccardo *et al*., 1974) and as a supporting/conjugate material in systems constructed to be functional in biological environments, for example, in biomedical, agricultural and wastewater treatment (Berger *et al*., 2004; Sakkayawong *et al*., 2005). Due to the presence of amino groups in its molecules,

1 Laboratory of Molecular Enzymology, Faculty of Research Agriculture, Hokkaido University, Kita 9, Nishi 9, Kita-ku, Sapporo, 060-8589, Japan.

2 Department of Microbiology, Faculty of Liberal Arts and Science, Kasetsart University, Kamphang Saen Campus, Nakhon Pathom 73140, Thailand.

3 Department of Science, Faculty of Liberal Arts and Science, Kasetsart University, Kamphang Saen Campus, Nakhon Pathom 73140, Thailand.

4 Graduate School of Environmental Science, Hokkaido University, Kita-ku, Sapporo, 060-0810, Japan.

5 Department of Biotechnology, Faculty of Agro-Industry, Kasetsart University, Bangkok 10900, Thailand.

6 Center for Advanced Studies in Tropical Natural Resources, National Research University-Kasetsart University, Kasetsart University, Bangkok 10900, Thailand. (CASTNAR, NRU-KU, Thailand).

* Corresponding author, e-mail: sarote.s@ku.ac.th

Received date : 22/06/12 Accepted date : 25/10/12

chitosan: (i) is a cationic polyelectrolyte (pKa ~ 6.5), (ii) is soluble in aqueous acidic media, (iii) forms water insoluble complexes with anionic polyelectrolytes and (iv) chelates metal ions (Li *et al.*, 1992). The solubility of chitosan in acidic solutions and the presence of hydroxyl and amino groups in its molecules are features relevant to the production of chitosan gels in a variety of configurations, especially beads (Krajewska, 2001). However, the use of chitosan solubilized in acid solution as living cell immobilization support has a limitation due to its bactericidal and fungicidal activity towards the ability to bind to the microbial outer membrane (Stössel and Leuba, 1984; Helander *et al*., 2001).

Synthetic dyes are used extensively by industries including paper printing and textile dying. The effluents of these industries are highly colored and disposal of these wastes into the environment can be extremely deleterious. In the case of azo and some other dye types, complete mineralization is difficult and the resulting aromatic amines may be toxic and display mutagenicity (Novotný *et al*., 2006). Consequently, considerable research effort has been devoted to optimizing color removal from solutions. Biosorption techniques are seen as an economic alternative with the main attractions of biosorption being high selectivity and efficiency, cost effectiveness and good removal performance (Kannan and Sundaram, 2001; Aksu, 2005).

Since many hydrophobic pollutants show a high tendency to accumulate onto microbial cells such as bacteria, fungi and algae, this biomass could be used as an adsorbent of biological origin for the removal of many hazardous organics from the wastewater. Moreover, this biomass can be cheaply and easily produced in rather substantial quantities (Kapoor and Viraraghavan, 1995). The term biosorption is used to indicate a number of metabolism-independent processes of physical and chemical adsorption, electrostatic interaction, ion exchange, complexation, chelation and microprecipitation taking place essentially in the cell wall rather than by oxidation though an anaerobic or aerobic metabolism (Aksu, 2005). The capability of uptake from aqueous solutions has been proven for heavy metals (Bailey *et al*., 1999), dyes (Yuzhu and Viraraghavan, 2001) and organic pollutants (Aksu, 2005).

Cell immobilization provides advantages over dispersed biomass as the former retains a higher biomass concentration, facilitates separation of the biomass from the pollutant-bearing solution and involves nondestructive recovery (Yuzhu and Viraraghavan, 2001). Chitosan can be produced chemically from chitin, (1→4)-2-acetamido-2-deoxy-β-glucan, and is second only to cellulose in terms of abundance in nature; it is found in the exoskeletons of crabs and other arthropods and in the cell walls of some fungi (Berkeley, 1979). Not only is chitosan inexpensive and abundant, it is also biologically inert, biodegradable and safe for humans and the environment (Muzzarelli, 1997). Because of these factors, its property of anti-microbial activity and instability of the bead form in acidic solution, therefore, there is a need to develop a technique of viable cell immobilization with chitosan. Previous research successfully demonstrated the production of macro spherical dried beads approximately 4 mm in diameter (Lang and Buranaboripan, 2007) and that the ionically acid-soluble chitosan gel could be used to entrap the fungal biomass initiate in the resting spore form and then be grown in culture media to produce exuberant mycelia for the removal of nonylphenol (an endocrine disrupting chemical) from aqueous solution (Langmuir adsorption isotherm constant (Q_0) = 312 $mg.g^{-1}$) as reported by Lang *et al*. (2009). Literature reviews have demonstrated the efficiency of general anionic dye and biomass under acidic conditions where there is resultant high interaction (Sakkayawong *et al*., 2005) and normal plain chitosan beads are not practical due to their instability in acid solution below pH 5.5 (Chiou *et al.*, 2004). Thus, the work reported in Lang and Buranaboripan (2007) and Lang *et al*. (2009) found the acid-tolerant

chitosan-immobilized *Rhizopus arrhizus* biomass (Ch-F beads) they produced had advantages over normal plain chitosan beads as they are very stable under acidic conditions, easily produced, had high biomass production and good removal performance.

The aim of the current article was to evaluate the potential of the Ch-F beads for their application in biosorption of the locally used industrial textile dyes—namely, typical azo (RR) and phthalocyanine chromophore (CT), respectively.

MATERIALS AND METHODS

Microorganism and cultivation

Five fungal strains—*R. arrhizus* TISTR 3606, *Trichoderma harzanum*, *Aspergillus oryzae*, *A. niger* and *Penicillium* sp.— were used and were obtained from the Microbiological Laboratory of the Faculty of Liberal Arts and Science, Kasetsart University. These were inoculated into tryptone glucose yeast (TGY) growth medium composed of 10 g yeast extract, 20 g peptone and 20 g dextrose for 1 L distilled de-ionized (DI) water, and cultivated in rotary shaking flasks at 30 ^{o}C for 5 d. *R. arrhizus* was grown on sterilized rice koji at 30 ^{o}C for 5 d for sporangiospore harvesting. The spores were prepared to 3.7×10^{9} spores.mL^{-1} as a stock spore suspension.

Dye stuff and chemicals

The two reactive textile dyes used in this study were obtained from a manufacturing unit of the local cotton textile industry (Kampaeng Saen Patana Co., Ltd., Nakhon Pathom, Thailand) in pure form and used without further purification. The dyes, RR (λ_{max} = 532 nm) and CT (λ_{max} = 667 nm) were manufactured by Dystar, Mumbai, India and Ciba Specialty Chemicals, Auckland, New Zealand, respectively. RR was classified as a vinylsulfone-based azo dyestuff but its color index (C.I.) number was unavailable. The C.I. number and chemical structure obtained for CT were 73049-92-0 and copper,[29H, 31H-phthalocyaninato (2-)-N_{29},N_{30},N_{31},N_{32}]-,sulfo[[4-[[2-(sulfooxy) ethyl]sulfonyl]phenyl]amino]sulfonyl derivative, respectively (Material Safety Data Sheet, 2003). Chitosan was purchased from Sigma-Aldrich (St. Louis, MO, USA). RR and CT dye were dissolved in distilled DI water to prepare a stock solution (1,000 mg.L^{-1}). The desired dye concentrations were obtained by successive dilutions.

Screening of dried fungal biomass for dye biosorption

Separate samples of the prepared mycelia of the above five fungal strains for screening were autoclaved (121.5 ^{o}C for 15 min) and harvested by filtering through a membrane filter. The harvested biomass was then washed thoroughly with DI water and freeze dried. The dried dead biomass was powdered using a mortar and a pestle. Particles passing through a 210 µm sieve were used as biosorbent for dye biosorption. Then, 0.2 g of each different dried fungal biomass (FB) was added to 20 mL RR and CT solution at pH 3.0 in 100 mL Erlenmeyer flasks and incubated with shaking (100 rpm) at 30 ^{o}C for 1 hr. The FB was separated by centrifugation at 10,000×*g* for 5 min at the end of incubation. The remaining dye in the supernatant was measured spectrometrically at 532 and 667 nm for RR and CT, respectively.

Preparation of acid-tolerant chitosan-immobilized *Rhizopus arrhizus* biomass (Ch-F beads), chitosan beads and dried fungal biomass

The immobilization of *R. arrhizus* sporangiospore via entrapment was carried out as Ch-F beads. Chitosan (3 g) was dissolved in acetic acid solution (3% volume per volume, 9 mL), heated at 100 ^{o}C for 10 min, cooled and then mixed with 1 mL of spore suspension. The fungal spore immobilized beads (approximately 2.5 mm in diameter) were cured in sodium tripolyphosphate solution (TPP, 2%, w/v) for 4 hr and then washed several times with distilled

DI water. The beads were then transferred in the TGY medium and incubated on a rotary shaker (100 rpm) at 30 °C. After incubation for 5 d, the Ch-F beads were killed by autoclaving (121 kPa, 121°C) for 15 min, removed from the medium by filtration, washed with distilled DI water and dried using a lyophilizer. The plain chitosan beads were treated as described above without the fungal spore entrapment. The FB powder of *R. arrhizus* was prepared according to the process for screening of the FB for dye biosorption, mentioned above.

Surface area measurement and biosorbent characteristics

The specific surface area of the Ch-F beads was determined using a Brunauer Emmett Teller (BET) surface area, the pore size, and pore size distribution (Poremaster 33; Quantachrome Instruments; Boynton Beach, FL, USA). The dried Ch-F beads were degassed by evacuation for 3 hr at 77.4 °C then the surface area was determined by the N_2 sorption method (Brunauer *et al*., 1983; Łyszczek and Lipke, 2013). The zeta potential was determined by an electro-acoustic technique with a Zeta Probe Analyzer (Zeta Meter 3.0; Malvern Instruments Ltd; Worcestershire; UK) at room temperature.

Batch biosorption studies

The biosorption of RR and CT onto the dried FB and Ch-F beads was carried out in a batch system. The effect of the solution pH and initial concentrations of the dyes on the biosorption capacity were studied. A stock solution (10 $g.L^{-1}$) of each dye was prepared by dissolving in distilled DI water. The optimal pH on the biosorption capacity of the FB was investigated in the pH range of 3.0–8.0 (which was adjusted with 1M HCl and NaOH) at 30 °C using an initial dye concentration of 50 $mg.L^{-1}$ in a rotary shaker rotated at 100 rpm. The effect of the initial dye concentration was studied at three different concentrations of each dye (50, 100, and 200 $mg.L^{-1}$) at pH 3.0. A series of 100 mL Erlenmayer flasks with 20 mg of biosorbent (either FB or Ch-F beads) in 20 mL of dye solution was shaken at 100 rpm at 30 °C. The supernatant was prepared by centrifugation at 10,000×*g* for 5 min and the remaining dye analyzed using UV/vis spectrophotometry at 532 and 667 nm for RR and CT, respectively. The results given in averages were obtained from the experiments repeated twice. The dye uptake was calculated using Equation 1:

$$q = \frac{(C_0 - C)V}{M} \quad (1)$$

where q is the dye uptake rate ($mg.g^{-1}$), C_0 and C are the initial and equilibrium concentrations of the dye ($mg.L^{-1}$), respectively, V is the volume of the aqueous phase (L) and W is the mass of dried cell used (g).

Biosorption isotherm

The initial dye concentration loaded on the FB or Ch-F beads was varied between 50 and 400 $mg.L^{-1}$ at the established optimum pH and incubated at 30 °C overnight. The dye uptake data were calculated and exploited for estimating the model parameters of the Langmuir and Freundlich isotherms. These estimations were performed using non-linear regression with Microsoft® Excel (Microsoft Corporation; Redlands, WA, USA), licensed to Kasetsart University.

Desorption

Saturated RR and CT-loaded Ch-F beads by the prior adsorption process were prepared, filtrated and washed with distilled DI water. The dye-loaded Ch-F beads were put into a shaking flask (120 rpm) containing HCl and NaOH solution (0.1 and 1.0 M) as eluent for 10 hr. The supernatant was taken and the absorbance measured at 532 and 667 nm for RR and CT, respectively. Desorption efficiency was measured using Equation 2:

Desorption efficiency (%) = Release dye (mg) × 100 / Initially absorbed dye (mg) (2)

Statistical analyses

The fit of kinetic expressions to the experimental data was tested using the value of the coefficient of determination, r^2 (Kumar, 2007), which is defined as:

$$r^2 = \frac{\sum(q_{cal} - \bar{q}_{exp})^2}{\sum(q_{cal} - \bar{q}_{exp})^2 + \sum(q_{cal} - q_{exp})^2} \quad (3)$$

where q_{cal} and q_{exp} are the theoretical and experimental dye uptake ($mg.g^{-1}$), respectively and $\bar{q}_{exp}$ is the average experimental dye uptake.

RESULTS AND DISCUSSION

Screening of fungal biomass

Five fungal strains that can produce asexual spores were used as the biomass sources for RR and CT biosorption since the fungi have prominent chitin layers in their cell walls and asexual spores. *A. niger*, *A. oryzae*, *Trichoderma* sp., *R. arrhizus* and *Penicillium* sp. showed dye removal percentages of 70, 86, 78, 98 and 66 for RR and 86, 74, 88, 92 and 82 for CT, respectively (data not shown here). The most effective FB was the mycelia of *R. arrhizus*; therefore it was selected as the fungal source for dye biosorption studies in this research. The inactive biomass of *R. arrhizus* has been also reported to be effective in the accumulation of Reactive orange 16, azo-dye class (O'Mahony *et al*., 2002).

Characterization of the dried fungal biomass and acid-tolerant chitosan-immobilized *Rhizopus arrhizus* biomass (Ch-F beads)

Since the original biomass powdered forms were unsuitable due to the difficulty of recovery and regeneration, the current research focused on the ionic interaction of immobilizing materials using TPP, the non toxic salt obtained from the triple condensation of PO_4 groups forming a gel and promoting the interaction between amino groups of chitosan and anionic groups of TPP (Aral and Akugba, 1998). Several attempts have focused on the improvement of the acidic and chemical stability of chitosan, such as using epichlorohydrin as a cross-linking agent for dye adsorption (Chiou *et al*., 2004). Nevertheless, there is no evidence of any reports on the modification of chitosan as a supporting material for good growth of living cells from a biosorption aspect. Earlier work by the current researcher successfully used chitosan as an immobilized material to produce a stable high density of biomass beads by using simple fermentation technique for nonylphenol uptake of 312 $mg.g^{-1}$ (Lang *et al*., 2009). The dried macro Ch-F beads (diameter approximately 4 mm, 9.7×10^{-4} g per bead) were completely different from the plain chitosan-TPP beads that had a diameter size of only 1.0–1.5 mm. The Ch-F beads were quite rigid and stabilized better than normal beads, with the latter being loose and tending to dissolve in the acid solution (Lang *et al.*, 2009). The specific surface area of the *R. arrhizus* FB was found to be 0.154 $m^2.g^{-1}$ with a particle size distribution of 5% below 20 μm, 5% below 95 μm and 90% below 250 μm. Scanning electron micrographs at 600× magnification of the Ch-F beads (Figure 1), prepared using the method of Pluemsab *et al*. (2007) shows the homogeneously distributed exuberant mycelia at the surface and the porosity of densely packed interior mycelia in the cross-section view. The physical characteristics of the Ch-F beads are indicated by: the BET surface area of the beads calculated by the physical adsorption of gas molecules, 151.90 $m^2.g^{-1}$; average pore size, 80.48 Å; %water absorption, 796.93; %apparent porosity, 95.84; bulk density, 0.12 $g.mL^{-1}$, and %apparent specific gravity, 2.9. The Ch-F beads formed a huge surface area larger than that obtained from *R. arrhizus* FB.

Biosorption pattern depending on the solution pH and type of reactive dyes

The fungal cell wall is composed of polysaccharides (chitin and chitosan), proteins, lipids with several functional groups (for example, amino, carboxyl, thiol and phosphate groups) capable of binding the dye molecules (Fu and

Viraraghavan, 2002; Bayramoglu and Arica, 2006). The ionic forms of the dye in solution and the surface electrical charge of the biomass depend on the solution pH. Therefore, the interaction between a dye and the biosorbent was mainly affected by the ionization states of the functional groups of both dye molecules and the biosorbent surface (Bayramoblu and Arica, 2006). The effect of pH on RR and CT on the FB in the range 3.0–8.0 is presented in Figure 2. The biosorption of both dyes increased at a more acidic pH. The maximum dye uptake value was found at pH 3.0 for both RR and CT. The uptake of CT, a pyrrole macrocyclic dye, was slightly decreased and remained at an almost constant value at an initial pH between 4 and 8. The biosorption of RR, azo dye, was found to be more pH dependent. The main functional groups of protonated fungal biomass are comprised of carboxyl, phosphate and amine sites. The negatively charged dye anions would exhibit electrostatic attraction towards the positively charged amine groups of the biomass surface. This coincides with the observation of Won *et al*. (2008) that the biosorption of reactive dyes onto the biomass was extremely dependent on the solution pH (Aksu and Tezer, 2005). Each biosorption material in the Ch-F beads was characterized by analysis of the surface charge of the FB and the chitosan beads (Figure 3). Zero point charge of FB was found at pH 4.6. The highest zeta potential value was 52.9 and 25.3 mV for the chitosan beads and FB, respectively. Both are comparable to the report of Das *et al*. (2007) that studied the biosorption of mercuric ions onto *Aspergillus versicolor* biomass. Their zeta potential decreased from +15.1 to -35.5 mV corresponding to an increase in the pH from 2.0 to 8.0 and the zero point charge being noted at pH 3.5. Though the zeta potential of the FB was highest at pH 4.0 (Figure 3), the optimum pH for

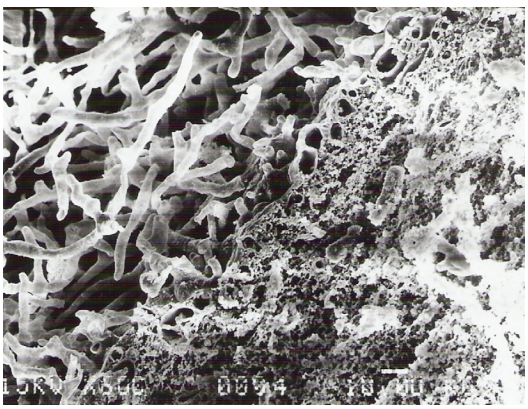

Figure 1 Scanning electron micrograph of the cross section detail of acid-tolerant chitosan-immobilized *Rhizopus arrhizus* biomass (Ch-F beads).

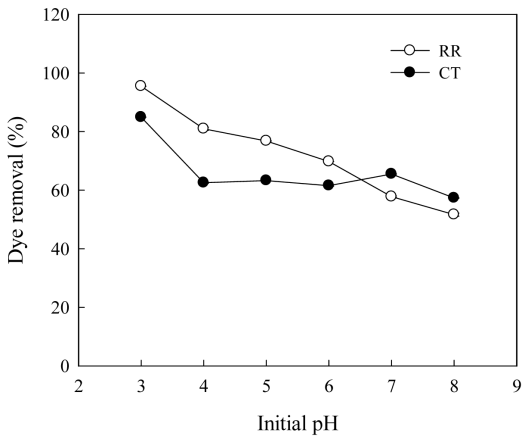

Figure 2 Effect of solution pH on the biosorption of Remazol Red RGB (RR) and Cibacron Turquoise HGN (CT) onto dried fungal biomass.

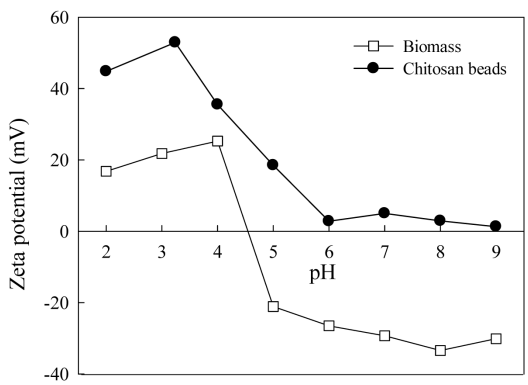

Figure 3 Surface charge characteristics of dried fungal biomass and chitosan beads.

adsorption of RR and CT was found to be at pH 3.0 (Figure 2) because at the lower pH, anionic dye becomes more negatively charged, which enhances attachment preferably (Figures 1, 2 and 3).

Kinetics of biosorption

It is important to investigate the mechanisms of biosorption and the potential rate controlling steps at which the dyes are removed from aqueous solutions by two types of Ch-F beads and FB. Two simplified kinetic equations—the pseudo first-order and pseudo-second order kinetic model—initially proposed by Lagergren (1989) and Ho and McKay (2000), respectively, have been used for a wide range of solute-sorbent systems. The pseudo-first order kinetic model of Lagergren's equation assumes that the biosorption rate is proportional to the number of unoccupied sites at the biosorption surface (Ozdemir *et al*., 2003). The kinetic model based on solid capacity can be formed using Equation 4:

$$q = q_e \left(1 - e^{-K_1 t}\right) \quad (4)$$

where q_e is the dye uptake rate at equilibrium (mg.g^{-1}), K_1 is the pseudo first-order rate constant (min^{-1}) and t is the contact time (min).

The pseudo-second order kinetic model of Ho's equation based on the sorption capacity of the solid phase assumes the driving force for the adsorption rate comes from the square of the difference between q and q_e (Ho, 2006). Equation 5 can thus be obtained:

$$q = \frac{q_e^2 K_2 t}{1 + q_e K_2 t} \quad (5)$$

where K_2 is the pseudo second-order rate constant modified (g.mg^{-1} min^{-1}).

The parameters of the kinetic models were estimated from the experimental data with the aid of a nonlinear curve-fitting approach. As seen in Table 1, the experimental data of both RR and CT dyes using the FB agree with the pseudo-second order kinetic model ascertained by the calculated correlation coefficient (r^2) in the range 0.992–0.999 for both RR and CT dyes. However, when the size and shape of the sorbent changed to the bead form, the experimental data became closer to the pseudo-first order kinetic model in the range 0.941–0.987 and 0.936–0.960 for the RR and CT dyes, respectively (Table 2). Based on these models, the curves are plotted in Figure 4. A large fraction of the dye was rapidly removed within 30 min of the contact time when

Table 1 Kinetic parameters of the pseudo-first order (Equation 4 in the text) and pseudo-second order rate (Equation 5 in the text) equations for the biosorption of Remazol Red RGB (RR) and Cibacron Turquoise HGN (CT) by dried fungal biomass.

Dye	C_0	q_{exp}	Pseudo-first order kinetic (Equation 4)			Pseudo-second order kinetic (Equation 5)		
			K_1	$q_{e,cal}$	r^2	K_2 (× 10^{-3})	$q_{e,cal}$	r^2
RR	52	52.1	0.146	52.1	0.989	9.79	51.7	0.999
	103	102.6	0.143	102.6	0.996	5.37	101.8	0.999
	167	152.3	0.023	151.7	0.990	0.34	141.0	0.992
CT	58	57.0	0.155	57.0	0.972	8.21	56.5	0.999
	66	64.1	0.105	64.1	0.994	5.01	63.3	0.999
	123	103.8	0.033	103.7	0.904	0.76	98.6	0.992
	178	124.3	0.023	123.7	0.857	0.30	111.7	0.998

C_0 = Initial concentrations of dye (mg.L^{-1}); q_{exp} and $q_{e,cal}$ = Experimental and theoretical dye uptake (mg.g^{-1}), respectively; K_1 and K_2 = Pseudo first-order rate constant (min^{-1}) and pseudo second-order rate constant modified (g.mg^{-1} min^{-1}), respectively; r^2 = Coefficient of determination.

Table 2 Kinetic parameters of the pseudo-first order (Equation 4 in the text) and pseudo-second order rate (Equation 5 in the text) equations for the biosorption of Remazol Red RGB (RR) and Cibacron Turquoise HGN (CT) by acid-tolerant chitosan-immobilized *Rhizopus arrhizus* biomass (Ch-F beads).

Dye	C_0	q_{exp}	Pseudo-first order kinetic (Equation 4)			Pseudo-second order kinetic (Equation 5)		
			K_1 ($\times 10^{-3}$)	$q_{e,cal}$	r^2	K_2 ($\times 10^{-3}$)	$q_{e,cal}$	r^2
RR	44	44.1	19.00	44.1	0.975	1.22	43.3	0.962
	93	92.8	7.48	92.8	0.971	0.20	88.3	0.949
	144	141.0	3.14	135.3	0.987	0.04	122.2	0.845
	252	193.2	2.44	177.1	0.964	0.02	158.5	0.789
	318	202.0	5.22	200.8	0.941	0.06	187.2	0.954
CT	31	26.9	5.59	26.5	0.959	0.46	24.3	0.934
	58	46.4	4.00	44.1	0.960	0.18	39.9	0.924
	89	61.0	3.95	57.9	0.937	0.14	52.5	0.992
	117	67.0	4.61	64.6	0.936	0.15	58.8	0.908

C_0 = Initial concentrations of dye (mg.L^{-1}); q_{exp} and $q_{e,cal}$ = Experimental and theoretical dye uptake (mg.g^{-1}), respectively; K_1 and K_2 = Pseudo first-order rate constant (min^{-1}) and pseudo second-order rate constant modified (g.mg^{-1} min^{-1}), respectively; r^2 = Coefficient of determination.

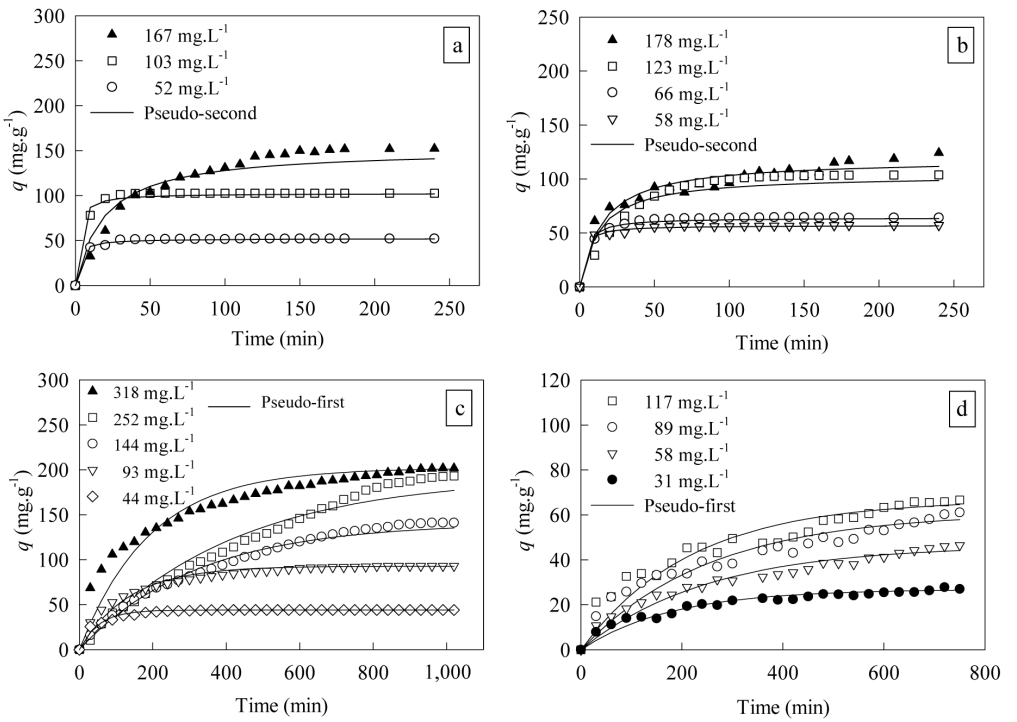

Figure 4 Biosorption kinetics by the FB described with the pseudo second-order model for Remazol Red RGB (RR) (a) and Cibacron Turquoise HGN (CT) (b) and by the acid-tolerant chitosan-immobilized *Rhizopus arrhizus* biomass (Ch-F beads) with the first-order model for RR (c) and CT (d).

using a low concentration of about 50 mg.L^{-1} dye absorbed onto the FB. Higher dye concentrations decreased the absorption rate but increased the dye uptake capacity in all the experimental variations studied.

Diffusion models

The intraparticle diffusion model identifies the diffusion mechanism well. Sorption kinetics is generally controlled by various factors including the following four steps: (i) bulk diffusion, (ii) film diffusion (external mass transfer), (iii) intraparticle diffusion and (iv) solute adsorption at active sites of the particle via the mechanisms of ion exchange, precipitation, complexation and/or chelation (Kannan and Karuppasamy, 1998). The intraparticle diffusion model is a single-resistance model in nature and can be derived from Fick's second law under two assumptions (Ruthven, 1984): (i) the intraparticle diffusivity, D is constant; and (ii) the uptake of sorbate by the adsorbent is small relative to the total quantity of sorbate present in the solution. The model assumes that the film diffusion is negligible and intraparticle diffusion is the only rate controlling step. The intraparticle diffusion model shown in Equation 6 implies that the diffusion from the surface to intraparticle sites is the only rate-limiting step (Weber and Morris, 1963; Yang and Al-Duri, 2005):

$$q = k_p t^{0.5} + C \quad (6)$$

where $t^{0.5}$ is the time required for the adsorbent to take up half as much adsorbate as it does at equilibrium, C is the concentration of dye (mg.L^{-1}) and k_p is the rate constant obtained from the slope of Equation 6 and is related to the intraparticle diffusivity by Equation 7:

$$k_p = \frac{6q_e}{R}\sqrt{\frac{D}{\pi}} \quad (7)$$

where D is the diffusion coefficient (cm^2.s^{-1}) and R is the radius of the bead (cm).

It is necessary to identify the steps involved during adsorption described by external mass transfer (boundary layer diffusion) and intraparticle diffusion and to determine which one is the rate-limiting step. The experimental data are determined in order to find the contribution of the rate controlling steps such as external mass transfer, intraparticle diffusion and the adsorption process. The values of k_{p1}, k_{p2} and correlation coefficients obtained from the slopes of straight lines are listed in Table 3. The plots of q against $t^{0.5}$ consist of two linear sections and their different slope values (k_{p1} and k_{p2}) for biosorption of the two dyes onto the FB can be seen in Table 3. The initial steep slope of k_{p1} indicates the instantaneous sorption of the dye molecules which may be due to chemisorption interactions at the surface of the biosorbent. The biosorption of RR and CT onto the FB showed a much larger k_{p1} value than that of the Ch-F beads. This first straight portion is attributed to the macro pore diffusion and the second linear portion to micro pore diffusion (Cheung *et al*., 2007). For the first step, about 80–90% of both RR and CT dyes was taken up by biomass within a $t^{0.5}$ value of 6.32 min. This is attributed to the instantaneous utilization of the most readily available adsorbing sites on the adsorbent surface. The second phase showed a gradual attainment of the equilibrium for the FB. This phase was described according to the report of Doğan *et al*. (2007) that this maybe attributed to a very slow diffusion of the adsorbates from the surface film into the micropores, which are the least accessible sites of adsorption. This also stimulates a very slow rate of migration of adsorbates from the liquid phase onto the adsorbent surface. However, it was still steeper for the Ch-F beads on biosorption of the RR dye. The RR dye uptake capacity showed an increasing trend up to 5–50% of initial q. Values of the intercept were observed only with the dye biosorption using the FB and were not seen using the Ch-F beads. This was in agreement with the report of Kannan and Sundaram (2001) regarding the thickness of the

boundary layer effect of powdered surfaces. In contrast, the plots of q versus the $t^{0.5}$ of CT dye onto the Ch-F beads would yield a straight line passing through the origin with the r^2 values in the range 0.84–0.98 (Table 3). This is consistent with the intraparticle diffusion that is controlling the rate.

Biosorption isotherm

Adsorption equilibrium

The capacity of an adsorbent can be described by the equilibrium sorption isotherm, which is characterized by certain constants whose values express the surface properties and affinity of the adsorbent.

Langmuir sorption isotherm

This model obtained under the ideal assumptions of a totally homogeneous adsorption surface, a finite number of binding sites and a few interactions between adsorbed molecules (Aksu and Balibek, 2007) is given by Equation 8:

$$q = \frac{Q_0 b C_e}{1 + b C_e} \quad (8)$$

where Q_0 is the Langmuir adsorption isotherm constant ($mg.g^{-1}$) and b is the Langmuir isotherm constant ($L.mg^{-1}$).

The Langmuir parameters can also be used to predict the affinity between the sorbate and sorbent using the constant dimensionless separation factor R_L, defined by Equation 9 (Hall *et al*., 1966):

$$R_L = \frac{1}{1 + b C_0} \quad (9)$$

where R_L is the constant separation factor.

The value of R_L can be used to predict whether a sorption system is in "favorable" or "unfavorable" equilibrium in accordance with the followed criteria: $0 > R_L > 1$ is favorable; $R_L > 1$ is

Table 3 Calculation of diffusivities of dyes in the dried fungal biomass (FB) and acid-tolerant chitosan-immobilized *Rhizopus arrhizus* biomass (Ch-F beads) using an intraparticle diffusion model.

Sorbent	Dye	C_0	k_{p1}	r^2	k_{p2}	r^2
FB	RR	52	3.172	0.915	0.098	0.678
		103	7.668	0.856	0.017	0.299
		167	22.09	0.992	9.041	0.984
Ch-F beads	RR	44	2.006	0.983	0.136	0.459
		93	4.682	0.986	1.274	0.890
		144	5.846	0.999	4.543	0.982
		252	6.282	0.988	7.509	0.994
		318	7.299	0.986	3.751	0.978
FB	CT	58	2.048	0.727	0.183	0.820
		66	4.630	0.942	0.169	0.539
		123	12.44	0.979	1.261	0.746
		178	5.735	0.876	4.593	0.916
Ch-F beads	CT	31	1.091	0.842	-	-
		58	1.733	0.977	-	-
		89	2.254	0.945	-	-
		117	2.588	0.916	-	-

CT = Cibacron Turquoise HGN; RR = Remazol Red RGB.

C_0 = Initial concentrations of dye ($mg.L^{-1}$), k_{p1} and k_{p2} = Rate constant ($mg.g^{-1}.min^{-0.5}$) obtained from the slope of Equation 6; r^2 = Coefficient of determination.

unfavorable; $R_L = 1$ is linear; $R_L = 0$ is irreversible. The R_L values for biosorption of RR and CT were calculated from the above expression are shown in Figure 5 and are in the range 0 to 1, indicating favorable uptake at all initial dye concentrations. However, the R_L values indicated that the CT uptake was less favourable for the Ch-F beads than FB.

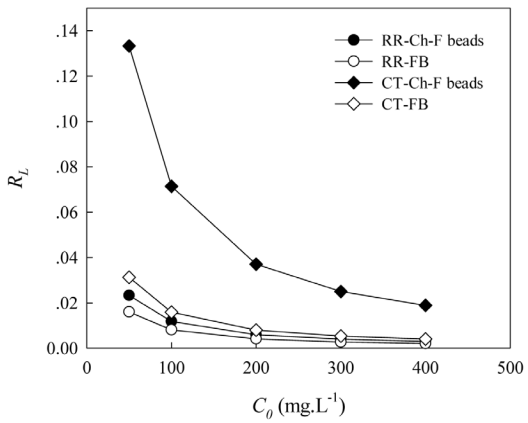

Figure 5 Value of separation factor, R_L for the biosorption of Remazol Red RGB (RR) and Cibacron Turquoise HGN (CT) by dried fungal biomass (FB) and acid-tolerant chitosan-immobilized *Rhizopus arrhizus* biomass (Ch-F beads).

Freundlich sorption isotherm

This model is suitable for a highly heterogeneous energetic distribution of active sites and interactions between adsorbed molecules and is defined by Equation 10 (Aksu, 2001):

$$q = K_F C_e^{1/n} \quad (10)$$

where K_F is the Freundlich constant, a characteristic of the system related to the adsorption capacity (mg.g^{-1}) and n is the constant characterizing the system related to the adsorption intensity.

Table 4 defines the total capacity of the biosorbents for two dyes. Two isotherms, the Langmuir and Freundlich adsorption isotherms, examined the fitness with biosorptive experimental data. The biosorption of RR and CT on the Ch-F beads and FB showed good agreement with the Langmuir equation (higher r^2) which could be explained by the surface area of the beads adsorbing the dye molecules at the mycelium monolayer. The Q_0 values that could be estimated from the Langmuir fit of RR and CT were 198.2 and 76.8 mg.g^{-1} for the Ch-F beads, and 162.42 and 120.7 mg.g^{-1} for the FB, respectively. These are comparable to previous reports; for example, Reactive orange 16 adsorbed by oven-dried *R.*

Table 4 Isotherm model constants of Remazol Red RGB (RR) and Cibacron Turquoise HGN (CT) absorbed onto dried fungal biomass (FB) and acid-tolerant chitosan-immobilized *Rhizopus arrhizus* biomass (Ch-F beads).

Constant	Ch-F beads		FB	
	RR	CT	RR	CT
Langmuir				
Q_0	198.2	76.8	162.4	120.7
b	0.84	0.13	1.23	0.62
r^2	0.958	0.999	0.958	0.998
Freundlich				
K_F	96.8	19.6	81.9	55.5
n	6.11	3.09	4.30	4.89
r^2	0.951	0.952	0.859	0.998

CT = Cibacron Turquoise HGN; RR = Remazol Red RGB.

Q_0 = Langmuir adsorption isotherm constant (mg.g^{-1}); b = Langmuir isotherm constant (L.mg^{-1}); K_F = Freundlich constant (mg.g^{-1}), n = Constant characterizing the system related to the adsorption intensity; and r^2 = Coefficient of determination.

arrhizus biomass with Q_0 = approximately 200 mg.g^{-1} (O'Mahony *et al.*, 2002), and Q_0 = 125 mg.g^{-1} for the biosorption of methylene blue by dead *Aspergillus fumigatus* (Abdallah and Taha, 2012). The biosorption of RR onto the Ch-F beads and FB was more effective than that of CT. This could have been due to a charge distribution of RR molecules that affects the interactions between the biomass binding sites better than the hydrophobic ring-shaped structure of CT.

Desorption

Desorption of RR and CT from the Ch-F beads with strong acidic and basic solutions demonstrated differences in the elution efficiency. The high acidity of the HCl solution showed an extremely low efficiency that ranged from 1.7 to 8.2% for the elution from the loaded beads (Figure 6). The optimum concentration of NaOH for desorption was 0.1 M which eluted 48.5–81.4% of the dyes from the loaded beads. RR-loaded beads showed previously more uptake but showed lower desorption efficiency compared to the CT pattern. This was considered to have resulted from the lack of uptake of CT observed at pH 3.0 due to physical electrostatic binding compared to RR. The regeneration and recovery capacity of the biomass exhibited a considerable decrease beyond the third cycle probably due to the remaining accumulated dyes.

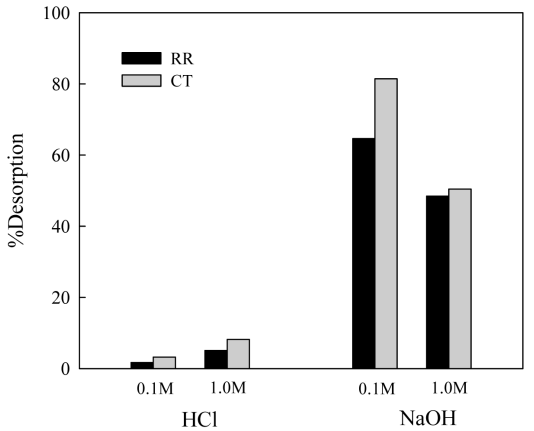

Figure 6 Desorption of Remazol Red RGB (RR) and Cibacron Turquoise HGN (CT)-loaded Ch-F beads eluted by 0.1 and 1.0 M HCl and NaOH.

CONCLUSION

The *R. arrhizus* mycelia were cultivated for the sole purpose of biomass harvesting without a high cost of production or a complicated preparation technique. The Ch-F beads were proven to be able to be used for dye biosorption and performed as a highly stable biosorbent in acidic conditions without any dissolution effect. The biosorption kinetics of the biomass in the bead form showed good agreement with the pseudo-first order kinetic model. The Ch-F beads showed a higher adsorption capacity for azo-chromophore dye and displayed a strongly electrostatic interaction pattern. Phthalocyanine-based dye showed a lower dye uptake capacity and the diffusion of the dye from the surface to intraparticle sites was considered as the rate-limiting step.

A dynamic flow mode operation will be conducted in the future to exploit the Ch-F beads for textile dye contaminated wastewater treatment.

ACKNOWLEDGEMENTS

This work was supported financially by the Kasetsart University Research and Development (KURDI), in 2008–2009 (W-T(D) 147.51). Additionally, the authors are grateful to the Higher Education Research Promotion and National Research University Project of Thailand, Office of the Higher Education Commission for partial financial support.

LITERATURE CITED

Abdallah, R. and S. Taha. 2012. Biosorption of methylene blue from aqueous solution by nonviable *Aspergillus fumigatus*. **Chem. Eng. J.** 195-196: 69–76.

Aksu, Z. 2001. Biosorption of reactive dyes by dried activated sludge: Equilibrium and kinetic modeling. **Biochem. Eng. J.** 7: 79–84.

Aksu, Z. 2005. Application of biosorption for the removal of organic pollutants: A review. **Process Biochem.** 40: 997–1026.

Aksu, Z. and E. Balibek. 2007. Chromium (VI) biosorption by dried *Rhizopus arrhizus*: Effect of salt (NaCl) concentration on equilibrium and kinetic parameters. **J. Hazard. Mat.** 145: 210–220.

Aksu, Z. and S. Tezer. 2005. Biosorption of reactive dyes on the green alga *Chlorella vulgaris*, **Process Biochem.** 40: 1347–1361.

Aral, C. and J. Akugba. 1998. Alternative approach to the preparation of chitosan beads. **Int. J. Pharm.** 168: 9–15.

Bailey, S.E, T.J. Olin, R.M. Bricka and D.D. Adrian. 1999. A review of potentially low-cost sorbents for heavy metals. **Water Res.** 33: 2469–2479.

Bayramoglu, G. and Y.M. Arica. 2006. Biosorption of benzidine based textile dyes "Direct Blue 1 and Direct Red 128" using native and heat-treated biomass of *Trametes versicolor*. **J. Hazard. Mat.** 143: 135–143.

Berger, J., M. Reist, M.J. Mayer, O. Felt, A.N. Peppas and R. Gurny. 2004. Structure and interactions in covalently and ionically crosslinked chitosan hydrogels for biomedical applications. **Eur. J. Pharm. Biopharm.** 57: 19–34.

Berkeley, R.C.W. 1979. Chitin, chitosan and their degradative enzymes, *In* R.C.W. Berkeley, G.W. Gooday and D.C. Ellwood, (eds.). **Microbial Polysaccharides and Polysaccharides.** Academic Press. London, UK.

Brunauer, S., P.H. Emmett and E. Teller. 1983. Adsorption of gases in multimolecular layers. **J. Am. Chem. Soc.** 60: 309–319.

Cheung, W.H., Y.S. Szeto and G. Mckay. 2007. Intraparticle diffusion processes during acid dye adsorption onto chitosan. **Bioresour. Technol.** 98: 2897–2904.

Chiou, S.M., Y.P. Ho and Y.H. Li. 2004. Adsorption of anionic dyes in acid solutions using chemically cross-linked chitosan beads. **Dyes Pigments** 60: 69–84.

Das, K.S., R.A. Das and K.A. Guha. 2007. A study on the adsorption mechanism of mercury on *Aspergillus versicolor* biomass. **Environ. Sci. Technol.** 41: 8281–8287.

Doğan, M., Y. Özdemir and M. Alkan. 2007. Adsorption kinetics and mechanism of cationic methyl violet and methylene blue dyes onto sepiolite. **Dyes Pigments** 75(3): 701–713.

Fu, Y. and T. Viraraghavan. 2002. Removal of Congo Red from an aqueous solution by fungus *Aspergillus niger*. **Adv. Environ. Res.** 7: 7239–7247.

Hall, K.R., L.C. Eagleton, A. Acrivos and T. Vermeulen. 1966. Pore- and solid diffusion kinetics in fixed bed adsorption under constant-pattern conditions. **Ind. Eng. Chem. Fund.** 5: 212–223.

Helander, I.M., E.L. Nurmiaho-Lassila, R. Ahvenainen, J. Rhoades and S. Roller. 2001. Chitosan disrupts the barrier properties of the outer membrane of Gram-negative bacteria. **Int. J. Food Microbiol.** 71: 235–244.

Ho, Y.S. and G. Mckay. 2000. The kinetics of sorption of divalent metal ions onto sphagnum moss peat. **Water Res.** 34: 735–742.

Ho, Y.S. 2006. Review of second-order models for adsorption systems. **J. Hazard. Mat.** B136: 681–689.

Kannan, N. and K. Karuppasamy. 1998. Low cost adsorbents for the removal of phenyl acetic acid from aqueous solution. **Indian J. Environ. Protec.** 18: 683–690.

Kannan, N. and M.M. Sundaram. 2001. Kinetics and mechanism of removal of methylene blue by adsorption on various carbons – a comparative study. **Dyes Pigments** 51: 25–40.

Kapoor, A. and T. Viraraghavan. 1995. Fungal biosorption-an alternative treatment option for heavy metal bearing wastewaters: A review.

Bioresour. Technol. 53: 195–206.

Krajewska B. 2001. Diffusion of metal ions through gel chitosan membranes. **React. Funct. Polym.** 47: 37–47.

Kumar, K.V. 2007. Pseudo second-order models for the adsorption of safranin onto activated carbon: Comparison of linear and non-linear regression methods. **J. Hazard. Mat.** 142: 564–567.

Lagergren, S. 1989. About the theory of so-called adsorption of soluble substances. **Kungliga Svenska Vetenskapsakademiens Handlingar**, Band 24: 1–39.

Lang, W. and W. Buranaboripan. 2007. **Method for Fungal Immobilization Using Chitosan as a Supporting Material.** Thai Patent, Application No. 7153.

Lang, W., C. Dejma, S. Sirisansaneeyakul and N. Sakairi. 2009. Biosorption of nonylphenol on dead biomass of *Rhizopus arrhizus* encapsulated in chitosan beads. **Bioresour. Technol.** 100: 5616–5623.

Li, Q., E.T. Dunn, E.W. Grandmaison and M.F.A. Goosen. 1992. Application and properties of chitosan. **J. Bioact. Compat. Polym.** 7: 370–397.

Łyszczek R. and A. Lipke. 2013. Microwave-assisted synthesis of lanthanide 2,6-naphthalenedicarboxylates: Thermal, luminescent and sorption characterization. **Micropor. Mesopor. Mat.** 168: 81–91.

Material Safety Data Sheet. 2003. **Chemical Information Net.** [Available from: http://www.chemcas.org/msds_archive/msds_01/cas/ga_msds/73049-92-0.asp]. [Sourced: 19 November 2012].

Muzzarelli, R.A.A. 1997. Human enzymatic activities related to the therapeutic administration of chitin derivatives. **Cell Mol. Life Sci.** 53: 131–140.

Novotný, Č., N. Dias, A. Kapanen, K. Malachova, M. Vándrovcová, M. Itävaara and N. Lima. 2006. Comparative use of bacterial, algal and protozoan tests to study toxicity of azo- and anthraquinone dyes. **Chemosphere** 63: 1436–1442.

O'Mahony, T., E. Guibal and M.J. Tobin. 2002. Reactive dye biosorption by *Rhizopus arrhizus* biomass. **Enzyme Microb. Technol.** 31: 456–463.

Ozdemir, G., T. Ozturk, N. Ceyhan, R. Isler and T. Cosar. 2003. Heavy metal biosorption by biomass of *Ochrobactrum anthropi* producing exopolysaccharide in activated sludge. **Bioresour. Technol.** 90: 71–74.

Pluemsab, W., Y. Fukazawa, T. Furuike, Y. Nodasaka and N. Sakairi. 2007. Cyclodextrin-linked alginate beads as supporting materials for *Sphingomonas cloacae*, a nonylphenol degrading bacteria. **Bioresour. Technol.** 98: 2076 – 2081.

Riccardo, A., A. Muzzarelli and R. Rocchetti. 1974. The use of chitosan column for the removal of mercury from waters. **J. Chromatogr.** 96: 115–121.

Ruthven, D.M. 1984. **Principles of Adsorption and Adsorption Processes.** Wiley. New York, NY, USA. 464 pp.

Sakkayawong, N., P. Thiravetyan and W. Nakbanpote. 2005. Adsorption mechanism of synthetic reactive dye wastewater by chitosan. **J. Colloid Interf. Sci.** 286: 36–42.

Stössel, P. and L.J. Leuba. 1984. Effect of chitosan, chitin and some aminosugars on growth of various soilborne phytopathogenic fungi. **J. Phytopathol.** 111: 82–90.

Weber, W.J. and J.C. Morris. 1963. Kinetics of adsorption on carbon from solutions. **J. Sanit. Eng. Div.** 89: 31–60.

Won W.S., H.M. Han and S.Y. Yun. 2008. Different binding mechanisms in biosorption of reactive dyes according to their reactivity. **Water Res.** 42: 4847–4855.

Yuzhu, F. and T. Viraraghavan. 2001. Fungal decolorization of dye wastewaters: A review. **Bioresour. Technol.** 79: 251–262.

Yang, X.Y. and B. Al-Duri. 2005. Kinetic modeling of liquid-phase adsorption of reactive dyes on activated carbon. **J. Colloid Interf. Sci.** 287: 25–34.